Korean J. Chem. Eng., **26**(6), 1580-1584 (2009)
DOI: 10.1007/s11814-009-0273-9

Effect of initial solution apparent pH on the performance of submerged hybrid system for the *p*-nitrophenol hydrogenation

Rizhi Chen*, Yan Du, Weihong Xing*, and Wanqin Jin*,†**

*State Key Laboratory of Materials-Oriented Chemical Engineering, College of Chemistry and Chemical Engineering, Nanjing University of Technology, Nanjing 210009, China
**College of Environmental Sciences, Nanjing University of Technology, Nanjing 210009, China
(*Received 2 March 2009 • accepted 4 May 2009*)

Abstract–Coupling nanocatalysis with ceramic membrane separation can solve the problem of nanocatalyst separation in situ from a reaction mixture. A submerged hybrid system combining nanocatalysis and ceramic membrane separation was designed for the liquid phase hydrogenation of *p*-nitrophenol to *p*-aminophenol, and the effect of initial solution apparent pH (pH_a) on the performance of submerged hybrid system was investigated in detail. It is demonstrated that as the initial solution pH_a is adjusted from 4.5 to 7.5, the catalytic stability of nano-sized nickel is remarkably improved, possibly because the formation of impurity on the nickel surface can be restrained at weak alkaline condition, while the catalytic activity and selectively almost do not change. The membrane permeability is not affected significantly by the initial solution pH_a.

Key words: Apparent pH, Hybrid System, Ceramic Membrane, *p*-Nitrophenol, Catalytic Hydrogenation, Nano-sized Nickel

INTRODUCTION

p-Aminophenol is an important intermediate in the preparations of analgesic and antipyretic drugs [1-4]. Direct catalytic hydrogenation of *p*-nitrophenol is considered as an efficient and environmentally friendly route to preparing *p*-aminophenol [5]. Raney nickel [6], nano-sized nickel [6] and several noble metals such as Pt/C [5] have been used as catalysts for this reaction. The catalytic properties of nano-sized nickel have been proven to be superior to those of Raney nickel in this reaction in our previous works [6]. However, the separation of nano-sized nickel particles from the reaction products creates another problem to be solved in practical applications [7]. A feasible approach to overcome this problem is to attach catalysts to a suitable substrate, but in that case, the effective surface area of the catalysts particles will be decreased. In fact, it is reported that catalysts in suspension have a better efficiency than those immobilized [8-10].

In our previous works, a side-stream hybrid system combining nanocatalysis and ceramic membrane separation was developed for the recovery of nano-sized nickel catalysts from reaction products during the hydrogenation of *p*-nitrophenol to *p*-aminophenol [7]. By using a ceramic membrane, the nano-sized nickel particles can be recovered completely. However, the nano-sized nickel particles were found to easily adsorb on the surface of pipeline, tank and membrane, which caused a decrease of catalyst concentration in the reaction slurry and led to the consequent decline in reaction rate and permeate flux of the membrane [7]. To overcome the problem, in the present research a submerged hybrid system was developed, where the ceramic membrane was submerged in the reactor. As a matter of fact, the submerged hybrid has been paid increasing attention recently due to its less loss of fine catalysts and energy costs compared to the side-stream hybrid system [11-13].

As the hydrogenation reaction process is coupled with the membrane separation process, any parameters affecting the reaction would also affect the membrane performance. It is well known that the solution pH influences not only the physical and catalytic properties of nickel catalyst but also the surface state of membrane. Therefore, in the paper, we attempted to investigate the effect of initial solution pH_a on the performance of the submerged hybrid system, including the hydrogenation reaction and the membrane filtration to find an initial solution pH_a with better catalytic properties and comparable membrane filtration performance.

EXPERIMENTAL

1. Catalyst Preparation and Characterization

The nano-sized nickel catalysts were prepared by the improved chemical reduction method in a continuous reactor according to Du et al. [6]. The typical preparation process was as follows. Solutions of nickel ion were prepared by dissolving analytical grade nickel sulfate hexahydrate ($NiSO_4 \cdot 6H_2O$) with distilled water in the dissolving tank equipped with a temperature-control system and an agitator. The temperature of nickel ion solutions was controlled at 85 °C. Hydrazine hydrate ($N_2H_4 \cdot H_2O$) was chosen as the reducing agent. The two solutions were instantaneously mixed and violently agitated in the premixer by controlling the flow rate ratio of the nickel ion solutions to the reducer solutions at 4 : 1 by using the metering pump. The nucleation process finished in a split second and the growth of the crystal nucleus proceeded in the tubular reactor. The resulting catalysts were collected in the product tank, washed with distilled water and ethanol, and finally dried in oven at 80 °C to get the black powders of nickel.

X-ray powder diffraction (XRD) patterns were obtained on a Bruker

†To whom correspondence should be addressed.
E-mail: wqjin@njut.edu.cn

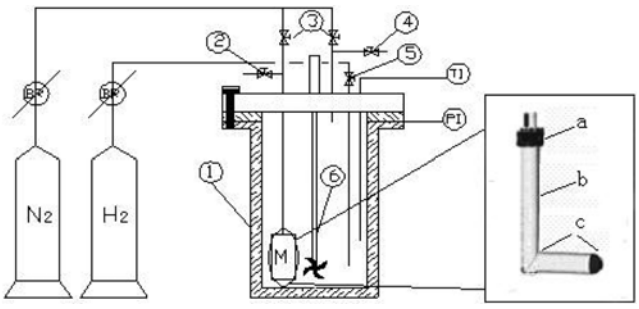

Fig. 1. Schematic diagram of the submerged hybrid system used for hydrogenation experiments.

1. Autoclave	PR. Pressure regulator
2. Liquid outlet valve	PI. Pressure indicator
3. Nitrogen inlet valve	TI. Thermocouple
4. Exhaust valve	a. Stainless subassembly
5. Hydrogen inlet valve	b. Ceramic membrane tube
6. Stirrer	c. Sealing
M. Membrane module	

D8 instrument with Ni-filtered Cu Kα radiation (λ=0.154 nm) at 40 kV and 30 mA, employing a scanning rate of $0.05^0 \cdot s^{-1}$ in the 2θ range from 20° to 80°. The morphology and particle size of the samples were observed by scanning electron microscopy (SEM, LEO-1530VP) and high-resolution transmission electron microscopy (HRTEM, JEM-2010). Specimens for HRTEM observations were sonicated in ethanol for 10 min and then loaded onto a copper fine gauze with carbon coatings.

2. Submerged Hybrid System

The submerged hybrid system, shown in Fig. 1, was designed and constructed in a laboratory-scale, which consisted mainly of a slurry stirred autoclave, a ceramic membrane module, hydrogen resource and nitrogen resource. The autoclave was made of stainless steel with a working volume of 2 L, which was equipped with an external heater and an internal thermocouple for temperature monitoring. The configuration of ceramic membrane module is also shown in Fig. 1. Asymmetric tubular ceramic membrane with 12 mm outer diameter, 8 mm inner diameter and a filtration area of 38 cm^2 was used in the experiments. The membrane was made up of a fine layer of α-Al_2O_3 with nominal pore size of 0.5 μm on the outwall of a tubular α-Al_2O_3 porous support, and was provided by Nanjing Jiusi High-Tech Co. Ltd., PR China. The preliminary experiments proved that the nano-sized nickel catalysts could be recovered completely by the ceramic membrane used due to the serious agglomeration of nickel particles as discussed in Section 3.1. The membrane was connected with the liquid outlet valve at one end; the other end was sealed by glaze.

3. Hydrogenation Experiments

The catalytic hydrogenation of *p*-nitrophenol to *p*-aminophenol over nano-sized nickel catalysts was carried out in the submerged hybrid system in batch operation. After 2 g catalysts and 35 g *p*-nitrophenol in 815 mL ethanol solution were introduced into the autoclave, the mixture was stirred until the *p*-nitrophenol was dissolved, and then the initial pH_a of the mother solution was unadjusted (pH_a=4.5) or adjusted to 7.5 by adding the appropriate amount of NaOH. The pH_a adjustment indicated that the mixture in the autoclave was changed to a new medium with a pH_a of 7.5. The previous works showed that at lower or higher initial solution pH_a the nano-sized nickel would obviously deactivate and no impurity formed on the surface of used nickel at initial solution pH_a greater than 2.5 [14]. Thus, at initial solution pH_a close to neutral, the nano-sized nickel may show better catalytic properties including catalytic activity and catalytic stability. The present research aims to find an initial solution pH_a with better catalytic stability and comparable catalytic activity. So in the present research only the two initial solution pH_a's of 7.5 and 4.5 were examined. The pH_a value of the mixture was measured with a PHS-3C pH meter (Shanghai Precision & Scientific Instrument CO., LTD, Shanghai, China). Calibration employed standard buffer solutions (pH 4.0, 6.86 and 9.18) before each pH_a measurement. After the pH_a measurement, the reactor was sealed and purged with nitrogen through the membrane tube six times to remove air and then purged with hydrogen six times. The reactor was heated to a desired temperature under low stirring. After the temperature reached the set value, the hydrogen was introduced into the reactor to a set level, and the reaction mixture was stirred at 800 rpm. The preliminary experiments proved that the hydrogenation reaction at stirring speed above 800 rpm was not influenced by external diffusion. Lastly, the hydrogenation reaction was performed at 102 °C and 1.65 MPa. After the hydrogenation reaction was finished, the reactor was cooled to 60 °C and the hydrogen was discharged. The reactor was then purged with nitrogen through the membrane tube six times to remove hydrogen. Subsequently, the membrane filtration was carried out at the nitrogen pressure of 0.25 MPa and the temperature of 60 °C. The nano-sized nickel catalysts were retained in the reactor and used repeatedly for the next hydrogenation reaction. Thus, the catalytic stability of nickel can be estimated, and the correlations between the catalytic stability and the times of nickel used repeatedly can be obtained. In this paper, the times of nickel used repeatedly is expressed by the number of catalytic reaction cycles, and the catalytic stability of nickel is expressed by the relative degree of catalyst deactivation defined by the ratio of the catalytic activity at certain reaction cycle to that at the first reaction cycle. The products were analyzed by an HPLC system (Agilent 1100 Series, USA) equipped with a diode array detector (DAD) and an auto-sampler. Chromatographic separations were performed at 35 °C with a ZORBAX Eclipse XDB-C18, 5 μm, 4.6 mm×250 mm column. A mobile phase composed of 80% methanol and 20% water at a flow rate of 1 $ml \cdot min^{-1}$ was used. The hydrogenation rate is expressed by the amount of hydrogen consumed per minute and per gram of catalyst [15], and the membrane permeability is expressed by the amount of the permeate per hour.

RESULTS AND DISCUSSION

1. Catalyst Characterization

The XRD pattern of the nano-sized nickel catalysts is shown in Fig. 2. Only three characteristic peaks of face-centered cubic (f.c.c.) nickel (2θ=44.5°, 51.9°, and 76.4°) marked by Miller index (1 1 1), (2 0 0), (2 2 0) can be observed in the 2θ range from 20° to 80°, suggesting the as-prepared samples are pure f.c.c. nickel. Some possible oxides such as NiO and Ni_2O_3 are not observed in XRD.

As shown in Fig. 3, the average particle size of the prepared nickel is about 20 nm. We can find from Fig. 4 that the nickel particles agglomerate seriously due to the comparatively small grain size and

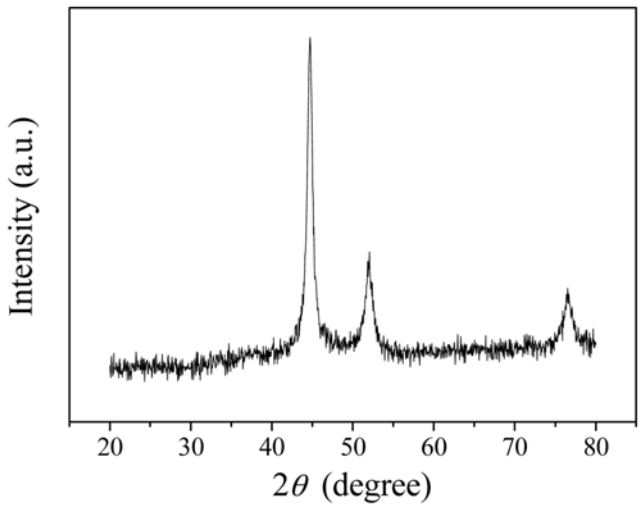

Fig. 2. XRD pattern of the nano-sized nickel catalysts.

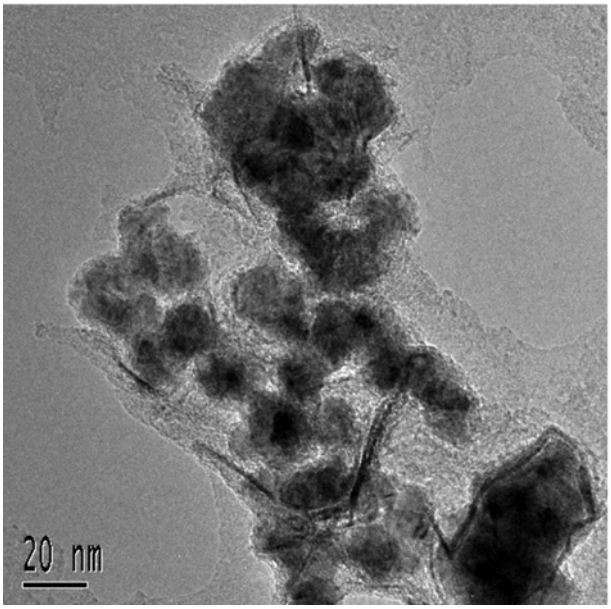

Fig. 3. TEM image of the nano-sized nickel catalysts.

the high surface energy.

2. Effect of the Initial Solution pH_a on the Catalytic Properties of Nano-sized Nickel

The effect of the initial solution pH_a on the hydrogenation rate of *p*-nitrophenol hydrogenation to *p*-aminophenol catalyzed by nano-sized nickel is presented in Fig. 5. The hydrogenation rate first increases with time and then becomes stabilized with respect to the *p*-nitrophenol hydrogenation at the two different initial solution pH_a values, respectively. The first stage corresponds to the activation of nano-sized nickel. Nickel oxide such as NiO or Ni_2O_3 can exist on the nickel surface due to the oxidation of nickel during the after-treatment [6]. Therefore, during the hydrogenation, these nickel oxides are first reduced by hydrogen to nickel, resulting in increasing the effective amount of nickel and the catalytic activity. The second stage is related to the concentration of *p*-nitrophenol, namely that the hydrogenation rate is not affected by *p*-nitrophenol concentration except at lower concentrations [5]. When the initial solution pH_a is adjusted from 4.5 to 7.5, the activation time increases obvi-

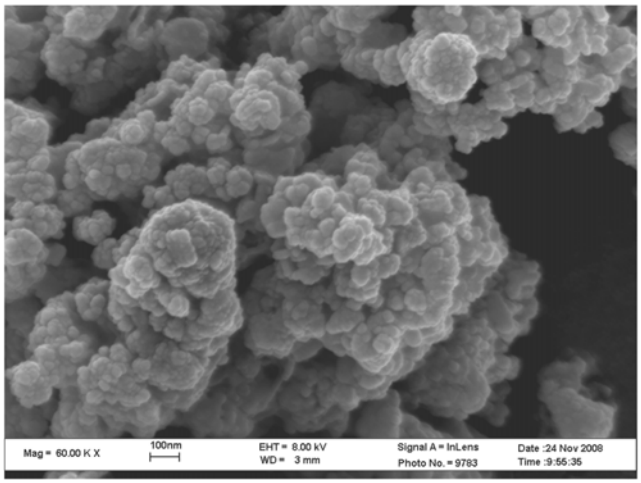

Fig. 4. SEM image of the nano-sized nickel catalysts.

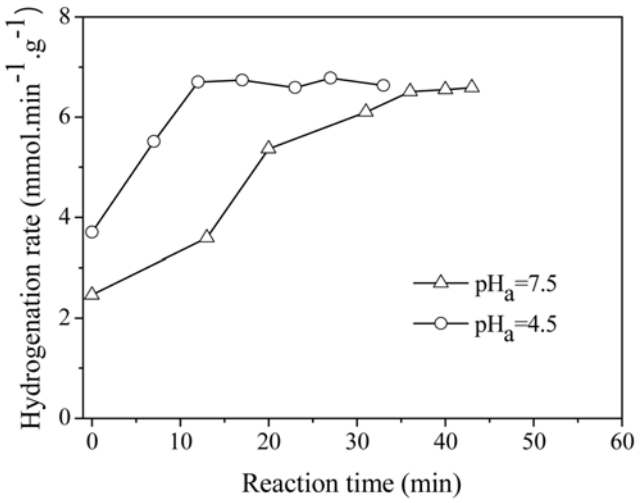

Fig. 5. Variation of hydrogenation rate of *p*-nitrophenol with time.

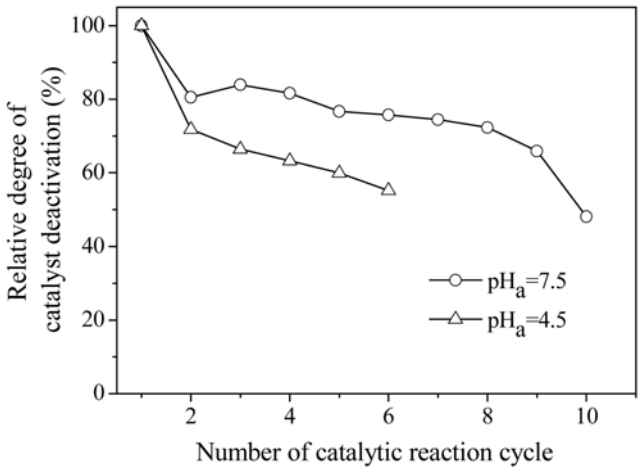

Fig. 6. Catalytic stability investigations of nano-sized nickel in the submerged hybrid system.

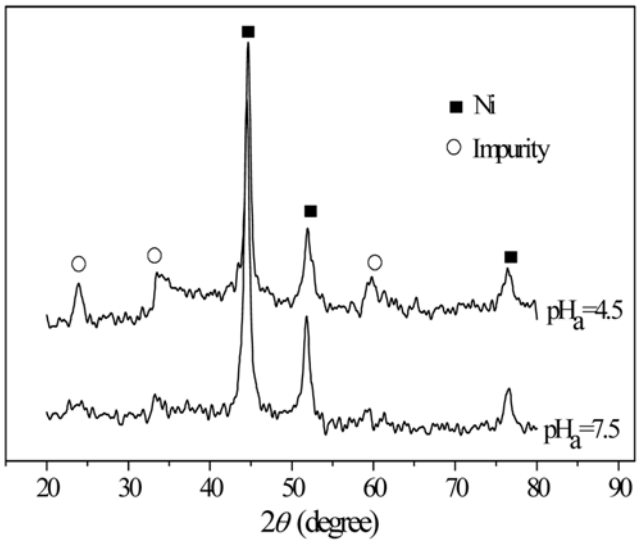

Fig. 7. XRD patterns of the used nano-sized nickel catalysts.

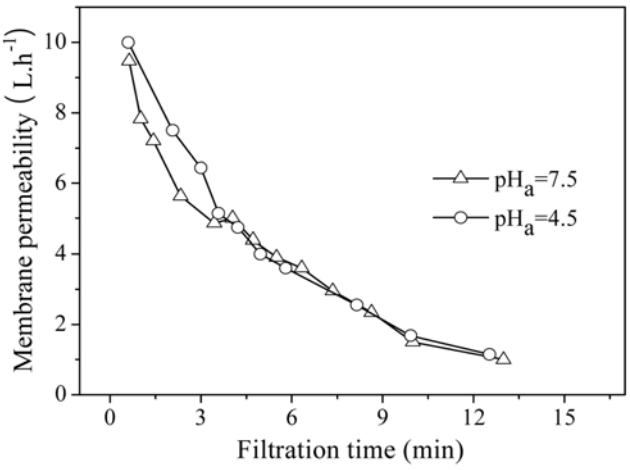

Fig. 8. Variation of membrane permeability with time.

ously, possibly because the increased hydroxyl ion could affect the activation of nano-sized nickel. It is also seen from Fig. 5 that when the hydrogenation rate becomes stabilized, the initial solution pH$_a$ almost has no influence on the catalytic activity of nano-sized nickel.

The correlations between the relative degree of catalyst deactivation and the number of catalytic reaction cycles are shown in Fig. 6. During each continuous *p*-nitrophenol hydrogenation cycle, nano-sized nickel is almost undergoing deactivation at the two different initial solution pH$_a$ values, respectively. It is interesting to find from Fig. 6 that when the initial solution pH$_a$ is adjusted from 4.5 to 7.5, the catalytic stability of nano-sized nickel is obviously improved. Throughout six continuous hydrogenation cycles, the nano-sized nickel at the initial solution pH$_a$=4.5 suffers 44.2% deactivation, while the nano-sized nickel at the initial solution pH$_a$=7.5 only suffers 34.1% deactivation throughout nine continuous hydrogenation cycles. To investigate the reason, the nano-sized nickel catalysts used were characterized by XRD, and the results are shown in Fig. 7. For the nickel used at the initial solution pH$_a$=4.5, the main composition is still elementary nickel (2θ=44.5°, 51.9° and 76.4°, corresponding to the Miller index (1 1 1), (2 0 0), (2 2 0), respectively) and at the same time some impurity peaks (2θ=23.8°, 33.2° and 59.3°) are obviously observed. The impurity adsorbed strongly on the surface of nano-sized nickel should be responsible for the lower catalytic stability of nickel used at the initial solution pH$_a$=4.5. Our previous works indicated that the impurity might be the complex compound of *p*-nitrophenol and nickel ion according to the analyses of XRD, ICP and FTIR [14]. When the initial solution pH$_a$ is adjusted from 4.5 to 7.5, the impurity peaks are almost not observed as shown in Fig. 7, indicating that the formation of impurity on the nickel surface could be restrained at weak alkaline condition. The phenomena can be explained as follows: during the continuous *p*-nitrophenol hydrogenation cycles, at the initial solution pH$_a$=4.5 some nickel particles were dissolved to form nickel ion and subsequently the nickel ion interacted with the *p*-nitrophenol to form a complex compound; while at the initial solution pH$_a$=7.5, almost no nickel ion formed and as a result the complex compound could not form. In our earlier works [14], for the nickel used at the initial solution pH$_a$ greater than 2.5, the composition is almost elementary nickel and no noticeable impurity peaks are observed from the XRD patterns of used nickel, possibly because the nickel sample was only used one time and no obvious impurity existed on the surface of used nickel. However, in the present study, at the initial solution pH$_a$=4.5, the nickel sample was used repeatedly six times and the used nickel was not cleaned after each *p*-nitrophenol hydrogenation; therefore some impurity could accumulate on the surface of used nickel and some impurity peaks can be observed from the XRD pattern of used nickel.

HPLC analysis results show that the initial solution pH$_a$ does not influence significantly the selectivity of the nano-sized nickel in the catalytic hydrogenation of *p*-nitrophenol to *p*-aminophenol.

3. Effect of the Initial Solution pH$_a$ on the Membrane Filtration Performance

Fig. 8 shows the variation of membrane permeability with filtration time. The membrane permeability decreases gradually with filtration time at the two different initial solution pH$_a$ values, respectively, because of a combination effect of the gradual increase of nickel catalysts concentration, the adsorption of nickel catalysts on membrane surface and the gradual decrease of filtration area during the concentration process of nickel catalysts suspension. It is seen from Fig. 8 that the membrane permeability in the primary stage of membrane filtration at the initial solution pH$_a$ of 7.5 is lower than that at the initial solution pH$_a$ of 4.5, possibly due because the nickel particles tend to disperse at higher pH$_a$ value and result in a cake consisting of fine particles, and as a consequence the filtration resistance increases and the flux decreases. As presented in Fig. 8, the influence of the initial solution pH$_a$ can be neglected at higher nickel concentration. Zhao et al. [16] also found that the flux of the ceramic membrane in the microfiltration of TiO_2 suspensions decreased as the pH value increased in a pH range of 2 to 10, which was attributed to the change of TiO_2 particle dispersity caused by increasing zeta potential.

Fig. 9 shows the correlations between the relative degree of membrane permeability (filtrating 400 mL reaction mixture) and the number of catalytic reaction cycles. The membrane permeability decreases obviously in the first three reaction cycles and then decreases slightly at the two different initial solution pH$_a$ values, respectively. This is

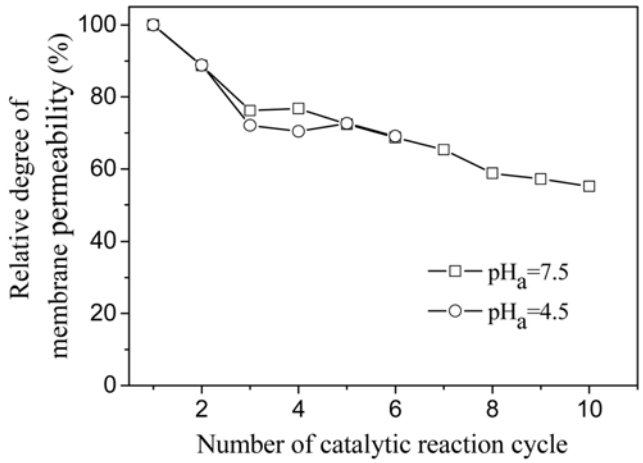

Fig. 9. Membrane permeability investigations in the continuous *p*-nitrophenol hydrogenation cycles.

because the adsorption of nano-sized nickel particles on the fresh membrane surface is obvious and the filtration resistance increases obviously; whereas, the adsorption of nano-sized nickel particles on the polluted membrane surface is weak and the filtration resistance increases slightly. As shown in Fig. 9, the initial solution pH_a has almost no influence on the membrane permeability in the continuous *p*-nitrophenol hydrogenation cycles.

CONCLUSIONS

A submerged hybrid system combining nanocatalysis and ceramic membrane separation was designed for the liquid phase hydrogenation of *p*-nitrophenol to *p*-aminophenol using nano-sized nickel as catalysts. Emphasis was given to the effect of initial solution pH_a on the performance of the submerged hybrid system. The initial solution pH_a has a great influence on the catalytic properties of nano-sized nickel, while almost no influence on the membrane permeability. When the initial solution pH_a is adjusted from 4.5 to 7.5, the activation time of nano-sized nickel increases obviously; however, the catalytic activity almost does not change. The catalytic stability of nano-sized nickel is obviously improved as the initial solution pH_a is adjusted from 4.5 to 7.5, possibly because the formation of impurity on the nickel surface could be restrained at weak alkaline condition. The initial solution pH_a does not significantly influence the selectivity of the nano-sized nickel.

Our study clarifies that the performance of the submerged hybrid system for the *p*-nitrophenol hydrogenation over nano-sized nickel catalysts could be improved by adjusting the initial solution pH_a from acidity to weak alkaline.

ACKNOWLEDGMENTS

Financial supports from the National Basic Research Program (2009CB623406), the National High Technology Research and Development Program (2007AA06A402) and the National Natural Science Foundation (20636020) of China are gratefully acknowledged.

REFERENCES

1. Y. Du, H. L. Chen, R. Z. Chen and N. P. Xu, *Chem. Eng. J.*, **125**, 9 (2006).
2. C. V. Rode, M. J. Vaidya, R. Jaganathan and R. V. Chaudhari, *Chem. Eng. Sci*., **56**, 1299 (2001).
3. C. V. Rode, M. J. Vaidya and R. V. Chaudhari, *Org. Process Res. Dev.*, **3**, 465 (1999).
4. R. Z. Chen, Y. Du, W. H. Xing and N. P. Xu, *Chin. J. Chem. Eng*., **14**, 665 (2006).
5. M. J. Vaidya, S. M. Kulkarni and R. V. Chaudhari, *Org. Process Res. Dev.*, **7**, 202 (2003).
6. Y. Du, H. L. Chen, R. Z. Chen and N. P. Xu, *Appl. Catal. A: Gen*., **277**, 259 (2004).
7. Z. X. Zhong, W. H. Xing, W. Q. Jin and N. P. Xu, *AIChE J*., **53**, 1204 (2007).
8. S. A. Lee, K. H. Choo, C. H. Lee, H. I Lee, T. Hyeon, W. Choi and H. H. Kwon, *Ind. Eng. Chem. Res*., **40**, 1712 (2001).
9. Y. B. Meng, X. Huang, Q. H. Yang, Y. Qian, N. Kubota and S. Fukunaga, *Desalination*, **181,** 121 (2005).
10. R. Thiruvenkatachari, S. Vigneswaran and I. S. Moon, *Korean J. Chem. Eng*., **25**, 64 (2008).
11. Q. Gan, S. J. Allen and G. Taylor, *Biochem. Eng. J*., **12**, 223 (2002).
12. J. K. Shim, I. K. Yoo and Y. M. Lee, *Process Biochem*., **38**, 279 (2002).
13. W. Yang, N. Cicek and J. Ilg, *J. Membr. Sci*., **270**, 201 (2006).
14. R. Z. Chen, Q. Q. Wang, Y. Du, W. H. Xing and N. P. Xu, *Chem. Eng. J*., **145**, 371 (2009).
15. Y. Du and R. Z. Chen, *Chem. Biochem. Eng. Q*., **21**, 251 (2007).
16. Y. J. Zhao, Y. Zhang, W. H. Xing and N. P. Xu, *Desalination*, **177**, 59 (2005).